Research Square

Preprints are preliminary reports that have not undergone peer review.
They should not be considered conclusive, used to inform clinical practice,
or referenced by the media as validated information.

# Investigation of Effects of Material Dimensions on Wrinkling in Flexforming Process

**Gürhan Yılgın** ( gurhanyilgin@gmail.com )
Turkish Aerospace Industries, Inc.
**Oguzhan Yilmaz**
Gazi University
**Fahrettin Ozturk**
Turkish Aerospace Industries, Inc.
**Hasan Ali Hatipoglu**
Turkish Aerospace Industries, Inc.

**Research Article**

**Keywords:** Flexforming, sheet forming, wrinkling, convex contour flange, contour structure.

**Posted Date:** February 12th, 2021

**DOI:** https://doi.org/10.21203/rs.3.rs-189051/v1

**License:** This work is licensed under a Creative Commons Attribution 4.0 International License.
Read Full License

## Abstract

Sheet metal forming processes are very common manufacturing and leading processes in automotive and aerospace industries. Flexforming is one of the sheet metal forming processes which is preferable due to its flexible manufacturing capabilities and its ability to produce multiple parts simultaneously. Convex contoured shaped parts are very much used in aerospace structures which are mostly produced by flexforming. Wrinkling is a characteristic defect for those kinds of parts. Prediction of wrinkling before manufacturing is highly crucial in order to reduce scrap rates, labor time, and other unexpected costs. In this research work, extensive amounts of experiments are conducted on flexforming press, and the process parameters such as material condition, contour radius, flange length, and material thickness which induce wrinkling are investigated in detail. Results have shown that sheet thickness is the most effective parameter, and as the sheet thickness is increased, wrinkling tendency is reduced extensively. Besides, increasing convex contour radius decreases wrinkling occurrence. Experimental findings are then used to generate wrinkling limit diagrams in which safety and failure zones are specified for different material conditions and sheet thicknesses. The developed diagrams might help to designer who can design defect free parts, reduce scrap rates, and reduce production costs significantly.

## 1. Introduction

The fundamental principal of hydroforming process is to apply pressurized fluid to a sheet to form a part [1]. Basically, pressurized fluid is used to form the part and a single die is generally used. In diaphragm forming (or flexforming), which is a special form of hydroforming, a force is produced by pressurizing fluid in a closed circle fluid system and this force is used to form the sheet. In the process, the sheet metal is placed onto a sheet metal die (usually the lower die) and the diaphragm including fluid reservoir is located at top. Then the fluid is pressurized and the diaphragm is moved towards the lower die. When the diaphragm is moved, the sheet is pressed between the diaphragm and the lower die. With the increase of pressure, the elastic diaphragm behaves like the upper die and the sheet metal is drawn into the lower die, completing forming process [2, 3].

Flexibility of the diaphragm accommodate multiple parts production due to its behavior like the upper die. For this reason, parts having different shapes can easily be manufactured [4]. It is a fact that aerospace industry has many different parts at limited quantity. Hereby, this method is widely used [5] and provide great advantages in terms of cost for aerospace industry. Parts produced by flexforming process have better surface qualities than the parts produced by other methods [6]. Besides, the usage of hydraulic pressure instead of the upper die, helps complex and difficult shaped parts production. In a conventional sheet metal forming operation, a die set containing an upper die and a lower die is needed, whereas in this method, only a lower die is sufficient. Elimination of the upper die and labor cost savings are the biggest advantageous of the process. Near to net shape geometry is almost achieved [7]. Thickness thinning is rather smaller with respect to conventional method and mostly homogeneous thickness distribution is obtained [8].

The common failure problem in flexforming is wrinkling. Wrinkling is a critical issue for sheet metal parts and developed generally in the wall or flange of the part. It is mostly seen in convex contour flanges because of sheet thickening or building up. The main reason is that the length of convex contour flange after production is much smaller than the original flange length [9].

Hatipoglu et al. [10] investigated the effect of some parameters, such as sheet thickness, die bend radius, flange length, and the rolling direction on forming of AA2024-T3 sheets both for straight and curved dies. The finite element model of the flexforming was constructed. They found that the flange length as well as the rolling direction for this aluminum alloy is seen to have insignificant effects on the springback, whereas the die radius and the sheet thickness have significant effects. Besides the finite element results were in an agreement with these experimental results. Abedrabbo et al. [11] studied the effect of contour radius on the wrinkling. They found that an increase in contour radius decreases wrinkling. Wang et al. [12] determined a mathematical model that shows the relationship between the flange length and strain. The results reveal that an increase in flange length raises wrinkles with a ratio. Sun et al. [13] experimentally studied the wrinkles occurred in rubber forming of convex shaped parts with Ti-15-3 material and examined them in finite element analysis. As a result of the study, they observed that the flange length and rubber have an effect on wrinkling. Liu et al. [14] examined the problem of wrinkling in hydroforming process both experimentally and finite element analysis. They determined the effect of material stress and diameter-thickness ratio of parts on wrinkling. Feyissa and Kumar [15] investigated the forming cryorolled AA5083 sheet material by hydroforming. They found out that parts with complex geometries formed by hydroforming method are more successful than the parts produced by conventional methods. Although wrinkling defect is critical for flexforming process, studies on this subject are limited. More investigation should be done.

In this research work, wrinkling problem for convex contour parts was investigated experimentally. The wrinkling behaviors of AA2024-O and AA2024-W by flexforming were determined for convex contour structures. Effects of thickness, flange length, and radius of convex contour on wrinkling in flexforming were investigated. The purpose of the research was to predict wrinkling before manufacturing. Otherwise, tremendous amount of effort and costs could be wasted. If the parameters that influence wrinkling are understood accurately, defect free parts can easily be manufactured. Designer can design the most accurate die with less modifications, and with less time and cost savings.

# 2. Materials And Method

## 2.1. Tensile Test

Tensile tests were performed in order to determine mechanical properties of sheet materials. All the tests were conducted by Zwick/Roell model Z100 machine with a 100 mm/min deformation speed at different directions. True stress vs. true strain diagrams for different alloy conditions were plotted in Fig. 1.

It is clearly seen that AA2024-W condition has higher strength than AA2024-O condition. The material was brought to W condition from O condition by heat treatment. W condition is an unstable intermediate condition which can also be observed in hardening behavior in the figure.

Mechanical properties such as yield strength, ultimate tensile strength, elongation, and anisotropy coefficients obtained from tensile tests are listed in Table 1.

Table 1
Mechanical properties of AA2024-O and AA2024-W alloys

| **Material** | ***YS*[*MPa*]** | ***UTS[MPa]*** | **ε** | $R_0$ | $R_{45}$ | $R_{90}$ |
|---|---|---|---|---|---|---|
| AA2024-O | 62 | 216 | 0,16 | 0,56 | 0,72 | 0,55 |
| AA2024-W | 148 | 423 | 0.18 | - | - | - |

# 2.2. Determination of Forming Limit Diagram

Forming Limit Diagram (FLD) provides failure limits at the onset of necking. For both aluminum alloy conditions, forming limit diagrams were determined. The FLDs were constructed using the Nakajima method [16]. The test samples were formed by a 600 kN Zwick model BUP 600 test machine. Deformations were measured optically and FLDs were plotted as seen in Fig. 2. The FLD results states that AA2024-O has better formability than AA2024-W which is also a well-known fact from shop floor practice.

# 2.3. Experimental Methods and Equipment

The purpose of experiments is to determine the effects of parameters which are mainly part dimensions on wrinkling tendency. All experiments were conducted at 70 MPa forming pressure with a constant oil temperature of 45°C, in 34°C ambient temperature. The total duration of forming process took about 3 min. and the part was exposed to maximum pressure for 3s. Experimental parameters, namely, material thickness (T), radius of contour (R), and flange length (F) are displayed in Fig. 3.

The experimental parameters were chosen to be the most effective ones on wrinkling and their ranges were determined by their incidences in aircraft parts designs. AA2024 is the mostly used material for flex formed parts and parts are formed either in O, or W condition. Therefore, both AA2024-O and AA2024-W were used in the experiments. Experimental parameters are summarized in Table 2. Bending radius of a constant value, 6.0 mm was selected.

Table 2
Parameters for the experiments

| Material conditions | AA2024-O | | | AA2024-W | |
|---|---|---|---|---|---|
| Material thickness, T (mm) | 0.63 | 1.27 | | 1.60 | 2.00 |
| Contour radius, R (mm) | 125 | 250 | 500 | 1000 | 2000 |
| Flange length, F (mm) | 30 | 40 | | 50 | |
| Bending radius (mm) | 6.0 | | | | |

Flat patterns of specimens were adjusted such that the desired flange lengths were obtained after the forming. Also for meaningful comparisons, specimen bending arc lengths (130 mm) are kept identical since they are very effective in wrinkle formation.

A single die was designed and manufactured for the experiments (Fig. 7a). This die was capable of forming all of the configurations in 24 runs (2 material x 4 thickness x 3 flange length). Specimens are attached on this die by the help of guide pins and then formed. Figure 7b shows formed specimens.

# 3. Results And Discussion

In this study, the effects of determined experimental parameters on flex formed parts were examined and compared Fig. 8 shows one of the formed specimens as a sample which has AA2024-W material, 1.27 mm thickness, 125 mm contour radius, and 40 mm flange length. As seen, two wrinkles were observed after forming.

The size of a wrinkle can be measured by two parameters which are height T, and width W (Fig. 9).

After performing the 24 runs, wrinkle sizes were measured and tabulated in Table 3. Some samples could not be measured due to their crushed forms.

Table 3
Wrinkling measurements

| Experiment No | Material | T (mm) | R (mm) | F (mm) | Number of wrinkles | $t_1$ x $w_1$ (mm) | $t_2$ x $w_2$ (mm) | $t_3$ x $w_3$ (mm) | $t_4$ x $w_4$ (mm) |
|---|---|---|---|---|---|---|---|---|---|
| 1 | Al2024-O | 0.63 | 125 | 20 | 1 | 0.82 x 3.48 | - | - | - |
| 5 | Al2024-O | 0.63 | 125 | 30 | 2 | 2.55 x 3.18 | 2.42 x 2.98 | - | - |
| | Al2024-O | 0.63 | 250 | 30 | 1 | 1.05 x 3.62 | - | - | - |
| 6 | Al2024-O | 1.27 | 125 | 30 | 2 | 2.18 x 7.25 | 1.81 x 7.11 | - | - |
| 7 | Al2024-O | 1.60 | 125 | 30 | 1 | 1.28 x 7.39 | - | - | - |
| 9 | Al2024-O | 0.63 | 125 | 40 | 3 | Not measured | 1.7 x 3.88 | 1.09 x 3.74 | - |
| | Al2024-O | 0.63 | 250 | 40 | 2 | 1.92 x 3.43 | 1.12 x 3.29 | - | - |
| | Al2024-O | 0.63 | 500 | 40 | 1 | 0.58 x 2.93 | - | - | - |
| 10 | Al2024-O | 1.27 | 125 | 40 | 2 | 3.27 x 5.93 | 2.47 x 6.77 | - | - |
| 11 | Al2024-O | 1.60 | 125 | 40 | 2 | 0.34 x 4.04 | 0.31 x 2.96 | - | - |
| 13 | Al2024-W | 0.63 | 125 | 20 | 4 | 1.84 x 4.91 | 1.36 x 5.07 | 1.43 x 4.71 | 1.03 x 4.26 |
| 14 | Al2024-W | 1.27 | 125 | 20 | 1 | 2.77 x 8.79 | - | - | - |
| 15 | Al2024-W | 1.60 | 125 | 20 | 2 | 2.28 x 11.53 | 0.94 x 8.71 | - | - |
| 16 | Al2024-W | 2.00 | 125 | 20 | 1 | 1.89 x 16.37 | - | - | - |

| Experiment No | Material | T (mm) | R (mm) | F (mm) | Number of wrinkles | t▯ x w▯ (mm) | t▯ x w▯ (mm) | t▯ x w▯ (mm) | t▯ x w▯ (mm) |
|---|---|---|---|---|---|---|---|---|---|
| 17 | Al2024-W | 0.63 | 125 | 30 | 3 | 3.34 x 4.04 | 3.24 x 3.22 | 1.20 x 4.44 | - |
| | Al2024-W | 0.63 | 250 | 30 | 2 | 2.33 x 4.21 | 1.26 x 4.48 | - | - |
| 18 | Al2024-W | 1.27 | 125 | 30 | 3 | 4.14 x 8.16 | 2.94 x 9.14 | 1.24 x 9.38 | - |
| 19 | Al2024-W | 1.60 | 125 | 30 | 1 | 5.67 x 9.63 | - | - | - |
| 20 | Al2024-W | 2.00 | 125 | 30 | 1 | 5.81 x 13.97 | - | - | - |
| 21 | Al2024-W | 0.63 | 125 | 40 | 2 | 4.18 x 2.97 | 3.77 x 4.42 | - | - |
| | Al2024-W | 0.63 | 250 | 40 | 2 | 2.54 x 3.73 | 2.19 x 4.31 | - | - |
| | Al2024-W | 0.63 | 500 | 40 | 1 | 1.69 x 4.07 | - | - | - |
| 22 | Al2024-W | 1.27 | 125 | 40 | 2 | 5.76 x 3.73 | 3.62 x 7.83 | - | - |
| | Al2024-W | 1.27 | 250 | 40 | 1 | 3.32 x 8.16 | - | - | - |
| 23 | Al2024-W | 1.60 | 125 | 40 | 1 | 7.34 x 6.71 | - | - | - |
| | Al2024-W | 1.60 | 250 | 40 | 1 | 2.19 x 10.75 | - | - | - |
| 24 | Al2024-W | 2.00 | 125 | 40 | 1 | 7.69 x 9.83 | - | - | - |

For better visualization, the flange edges of specimens were drawn on plots in Fig. 10–13. Those plots show the effects of experimental parameters on wrinkling clearly.

In Fig. 10, one can see the effect of sheet thickness on wrinkling. As the sheet gets thicker, the number of wrinkles decreases, and the size of wrinkles get bigger, and they disappear eventually Wrinkling phenomena can be thought as a sort of buckling in which thicker structures resist more.

Figure 11 shows the effect of flange length on wrinkling. Number of wrinkles increases as the flange length is increased. The reason behind this trend can be explained by considering the arc length of flange edge before and after forming. Before forming, in which the part was flat, the arc length of flange edge was higher than in its final form. As flange length increases, this difference gets higher in which more material is forced to take the final shape, resulting more compressive stresses and more wrinkle formations inevitably.

In Fig. 12, specimens bent in different contour radiuses are seen. As contour radius gets larger, wrinkle severity decreases. Again the reason can be explained by referring to previous discussion about the change in arc length of flange edge before and after bending. The change becomes insignificant as contour radius gets larger, converging zero in straight bending, which is wrinkle-free.

The effect of alloy condition on wrinkling is significant. Figure 13 shows the difference between W and O conditions of AA2024 for a specific configuration W condition, which is harder, has a wrinkle, whereas O condition is flawless. The reason is W is a heat treatment condition in which grains are small and homogeneous but they are also unstable causing bigger wrinkles on the formed part.

Above plots clearly reveal that at higher contour radiuses, wrinkles disappear, and when the flange length is increased, they appear again. The thickness is a positive effect on reducing wrinkles.

The aim of this study was to represent the experiment results in the form of wrinkling limit diagrams (WLD). These diagrams will provide safety and failure zones for a given geometry and material. Figure 14 shows a sample WLD for AA2024-O, 0.63 mm. The abscissa is contour radius, and the ordinate is flange length. Experiment results were plotted as dots. When sorted those dots as wrinkle - no wrinkle, a wrinkling limit curve may be fitted. The region above this curve is failure zone, and below is safety zone. This curve could be defined mathematically as:

$$y = 14{,}427\ln(x) - 49{,}658$$

This equation can be used to find wrinkling results of different configurations, and is also useful for configurations not found in the experiments. Similar diagrams were drawn for all the other materials and thicknesses.

One can see safe and wrinkling zone on the above graph. The curve on the graph form a border between safe and wrinkling zones. In the safe zone, no wrinkling should be observed. Similar graphs can be constructed based on material types and thicknesses. A designer may use those graphs effectively to find the optimum conditions.

# 4. Conclusions

In this study, the wrinkling defect in flexforming process was investigated experimentally. Aluminum alloy conditions, sheet thicknesses, contour radiuses, and flange lengths were considered as experimental parameters. Following results were drawn:

1. Sheet thickness was very effective on wrinkling. As the sheet thickness is increased, the wrinkling tendency is reduced significantly.
2. Contour radius of the bend was another effective parameter. As the contour radius is increased, wrinkle sizes get smaller, and when further increased, wrinkles disappear eventually.
3. Increasing flange length contributes to material thickening, therefore increases the risk of wrinkling.
4. Some combinations of experimental parameters provide wrinkle-free parts. Those results are used to generate wrinkling limit diagrams in which safety and failure zones are separated by a curve. At the end, those wrinkling limit diagrams can be used as a check tool by the designer.

# Declarations


### Acknowledgements

The authors sincerely thank Turkish Aerospace Industries, Inc. (TUSAŞ), Ankara, Turkey for supporting this work.


### Data availability

The datasets generated during and/or analysed during the current study are available from the corresponding author on reasonable request.


### Funding

This work was supported by Turkish Aerospace Industries, Inc. (TUSAŞ), Ankara, Turkey.


### Author information


### Affiliations

**Turkish Aerospace Industries, Inc., Ankara, Turkey**

Gurhan Yilgin, Hasan Ali Hatipoglu

**Advanced Manufacturing Technologies Research Group (AMTRG), Department of Mechanical Engineering, Gazi University, 06570, Maltepe, Ankara, Turkey**

Oguzhan Yilmaz

**Turkish Aerospace Industries, Inc., Ankara, Turkey & Department of Mechanical Engineering, Ankara Yıldırım Beyazıt University, Ankara, Turkey**

Fahrettin Ozturk

### Contributions

All authors contributed equally to the generation and analysis of experimental data, and the development of the manuscript.

### Corresponding author

Correspondence to Gurhan Yilgin.

### Compliance with ethical standards

### Ethics declarations

### Competing interests

The authors declare that they have no competing interests.

### Ethical approval

This work does not contain any ethical issues or personal information.

### Consent to participate

No human or animal was involved in this work; thus, no consent was required.

### Consent to publish

All authors have given their permission for publishing this work.

## References

1. Vahl M, Bobbert S, Hein P (2000) Hydroforming of sheet metal pairs for the production of hollow bodies. La Revue de Métallurgie 97, October: 1255–1263
2. Sala G (2001) A numerical and experimental approach to optimise sheet stamping technologies: part II—aluminium alloys rubber-forming. Mater Des 22:299–315
3. Davidson A (ed) (2016) Handbook of Precision Engineering, vol 10. Macmillan International Higher Education, London, pp 144–150
4. Ramezani M, Ripin ZM (2012) Rubber-Pad Forming Processes: Technology and Applications. Elsevier, Cambridge, pp 1–12
5. Kumar A, Kumar S, Yadav DR (2014) Review of rubber based sheet hydro-forming processes. In 5th International and 26th All India Manufacturing Technology, Design and Research Conference (AIMTDR), Guwahati, Assam
6. Kulkarni SM, Ruiwale VV, Jadhao MS, Kadam AA, Kale SR (2017) A review on Hydroforming Processes. International Journal of Current Engineering and Technology, 160–163

7. Bakhshi-Jooybari M, Gorji A, Elyasi M (2012) Developments in sheet hydroforming for complex industrial parts. Metal Forming-Process, Tools, Design. IntechOpen
8. Önder E, Tekkaya AE (2008) Numerical simulation of various cross sectional workpieces using conventional deep drawing and hydroforming technologies. Int J Mach Tools Manuf 48:532–542
9. Lee MG, Kim C, Pavlina EJ, Barlat F (2011) Advances in sheet forming—materials modeling, numerical simulation, and press technologies. J Manuf Sci Eng 133(6):061001
10. Hatipoğlu HA, Polat N, Koksal A, Tekkaya AE (2007) Modeling flexforming (fluid cell forming) process with finite element method. Key Eng Mater 344:469–476
11. Abedrabbo N, Zampaloni MA, Pourboghrat F (2005) Wrinkling control in aluminum sheet hydroforming. Int J Mech Sci 47:333–358
12. Wang CT, Kinzel G, Altan T (1995) Failure and wrinkling criteria and mathematical modelling of shrink and stretch flanging operations in sheet-metal forming. J Mater Process Technol 53:759–780
13. Sun YN, WAN M, Wu XD (2013) Wrinkling prediction in rubber forming of Ti-15-3 alloy. Trans Nonferrous Met Soc Chin 23(10):3002–3010
14. Liu G, Peng J, Yuan S, Teng B, Li K (2015) Analysis on critical conditions of sidewall wrinkling for hydroforming of thin-walled tee-joint. Int J Mach Tool Manu 97(97):42–49
15. Feyissa FT, Kumar DR (2019) Enhancement of drawability of cryorolled AA5083 alloy sheets by hydroforming. Journal of Materials Research Technology 8:411–423
16. Dilmec M, Halkaci HS, Ozturk F, Turkoz M (2012) Detailed investigation of forming limit determination standards for aluminum alloys. J Test Eval 41(1):1–12


# Figures

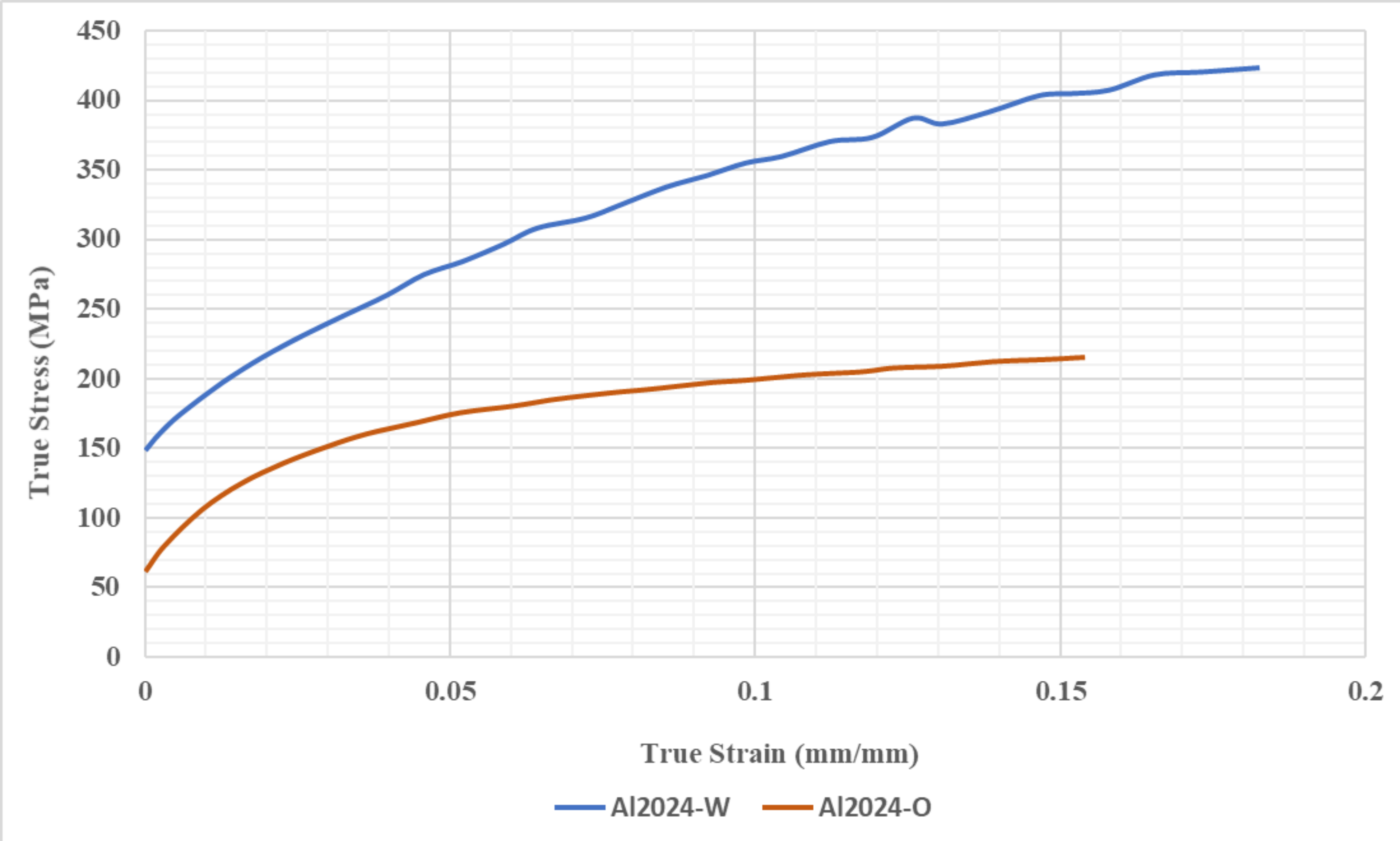


Figure 1

True stress vs. true strain diagrams for AA2024-O and AA2024-W

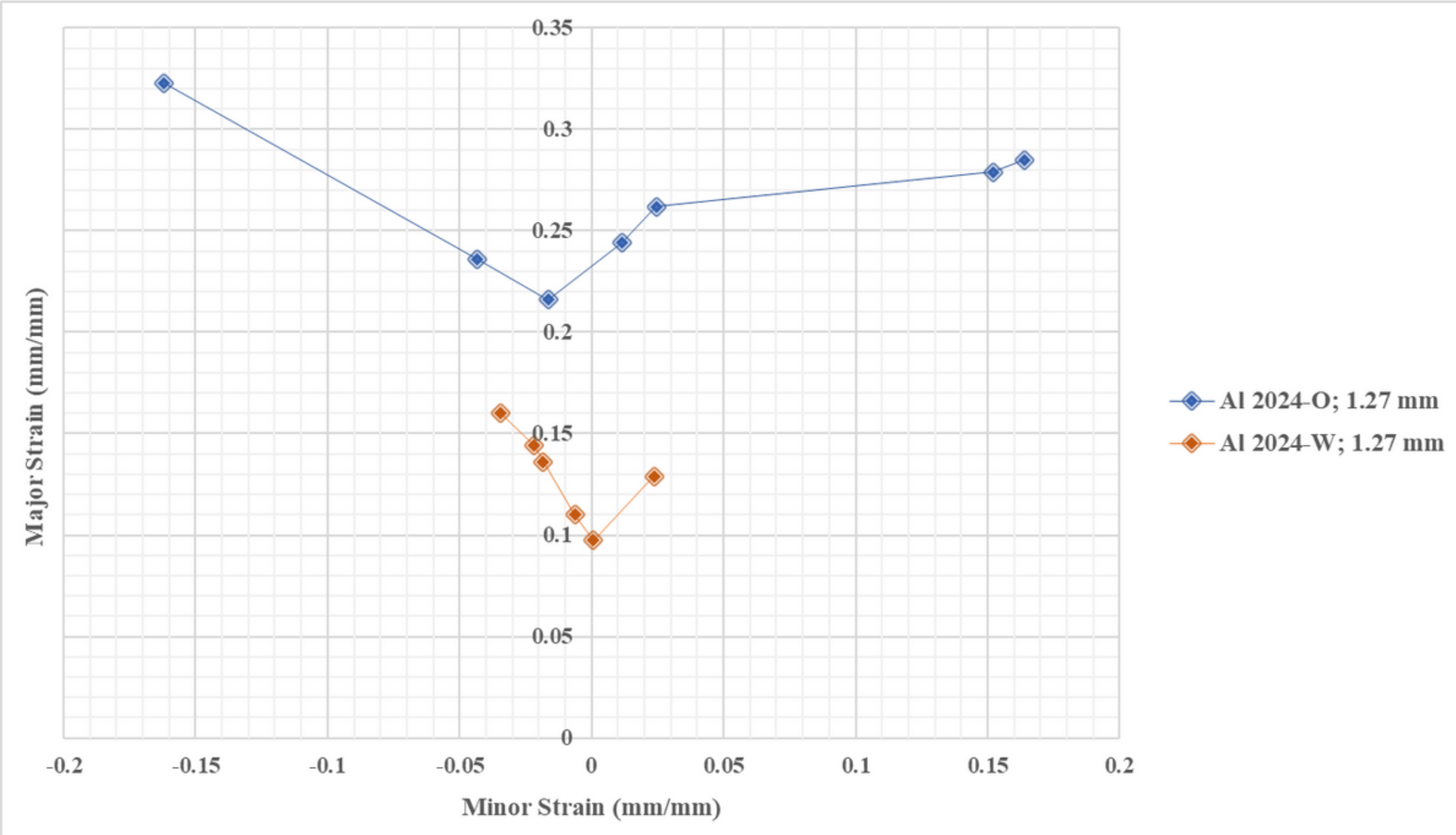


## Figure 2

Forming limit diagrams of AA2024-O and AA2024-W

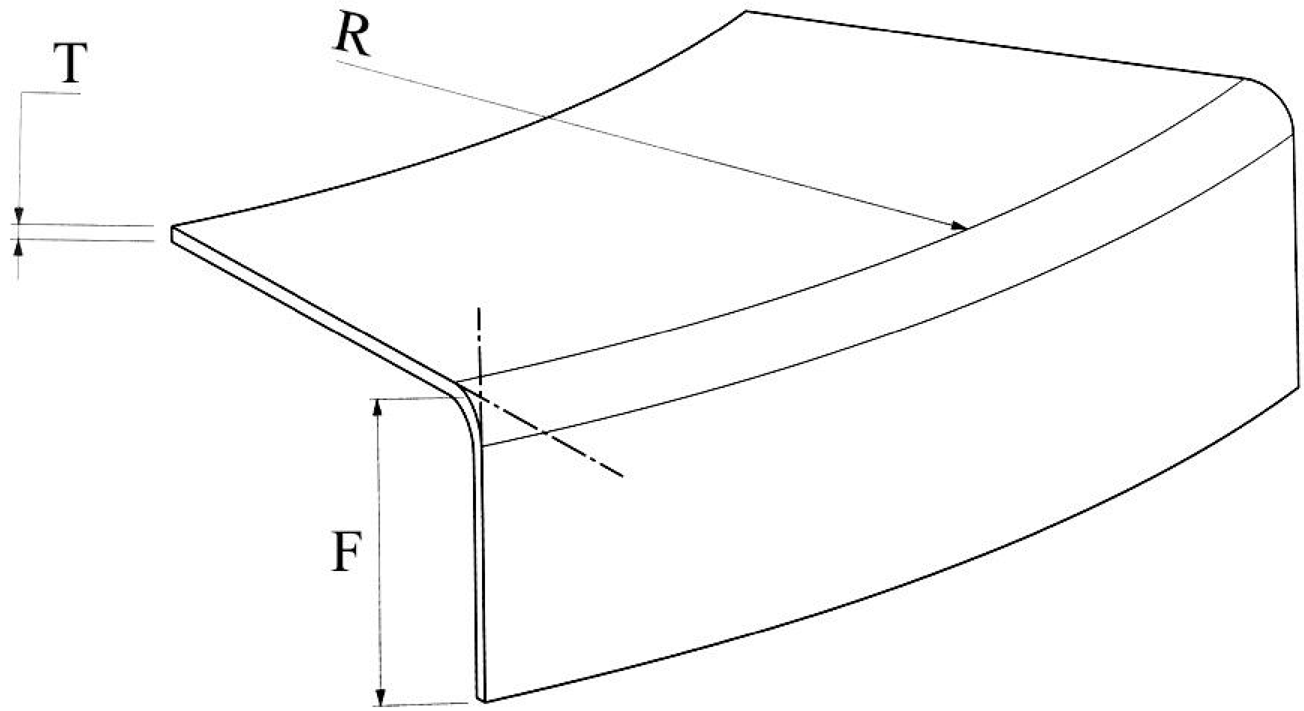


Figure 3

Schematic view of dimensional parameters used in the experiments

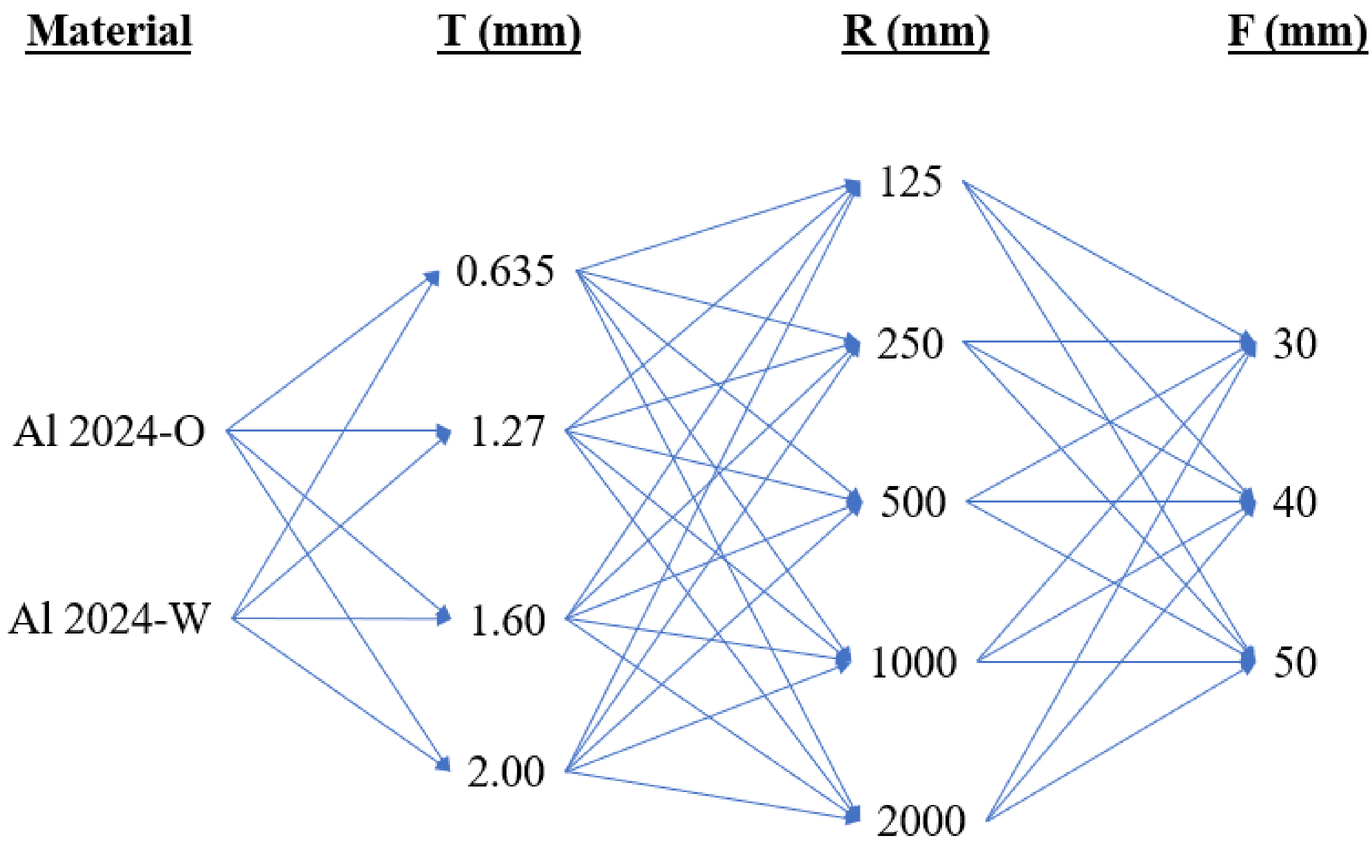


**Figure 4**

Experiments configuration

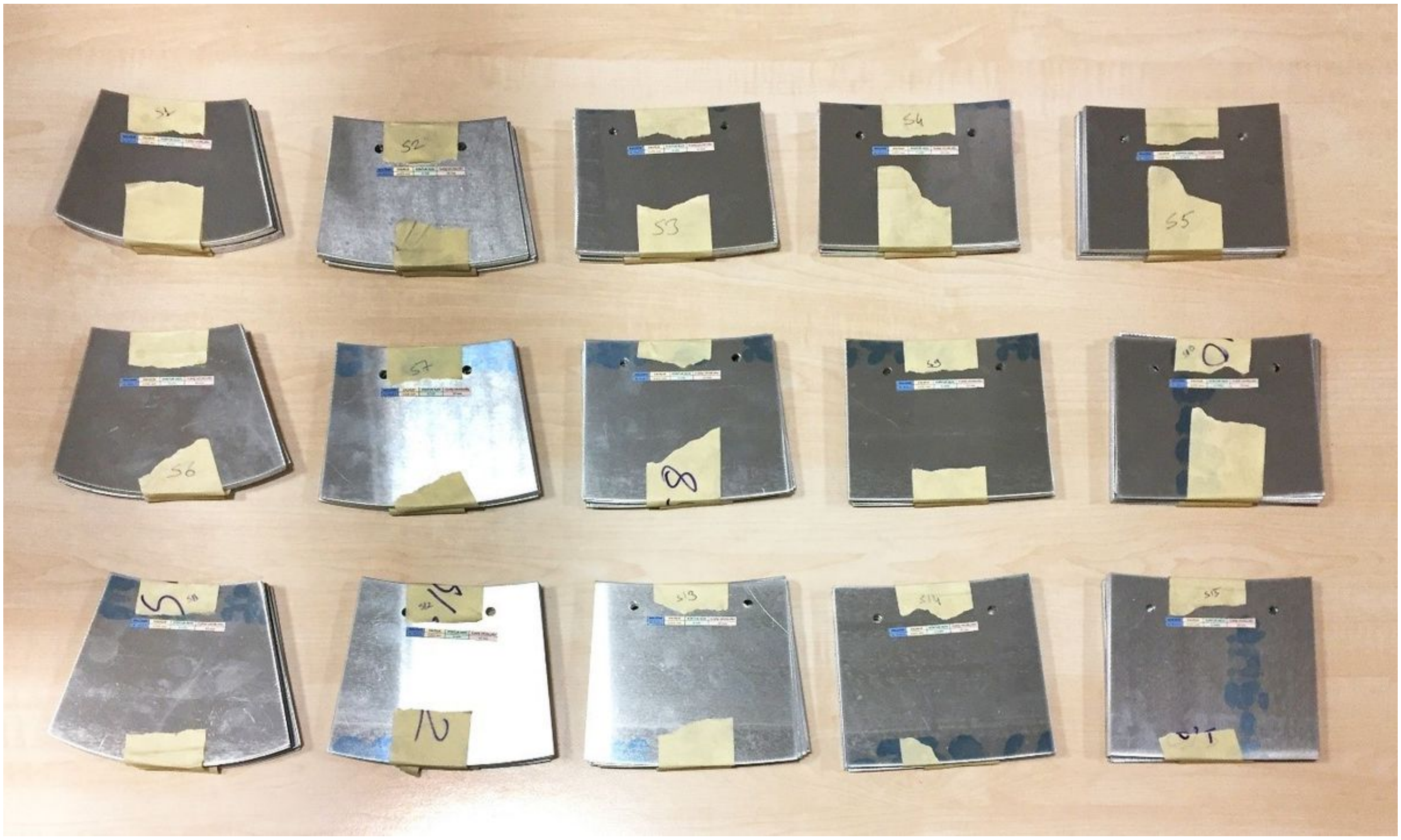

**Figure 5**

Specimens used in the experiments

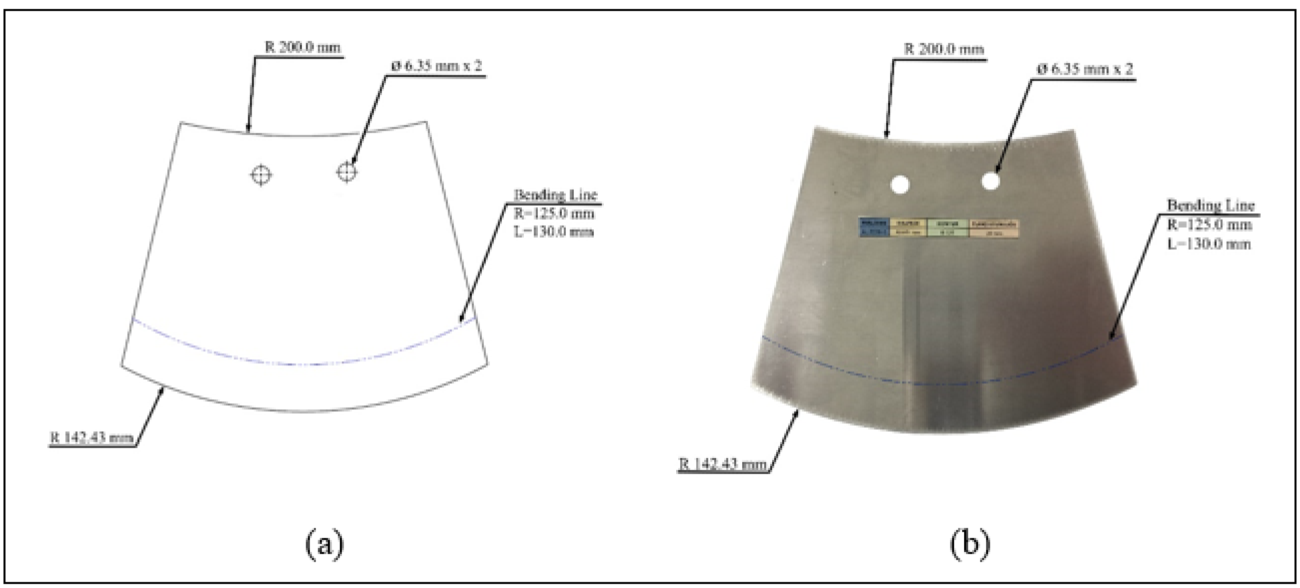


**Figure 6**

a) Schematic of a test sample geometry b) An example of test samples

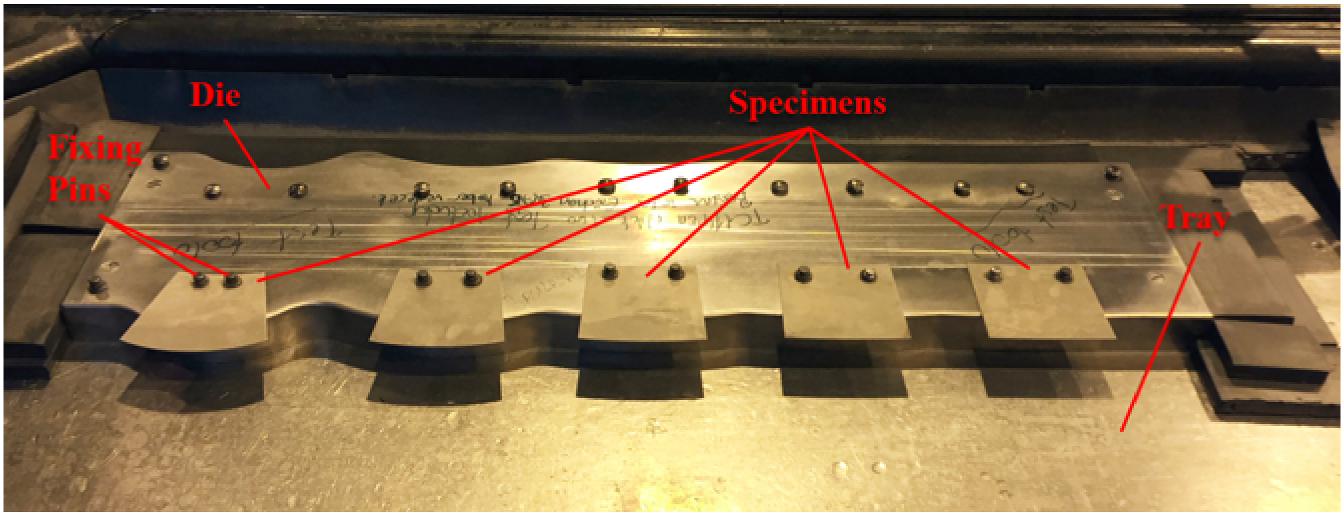


(a)

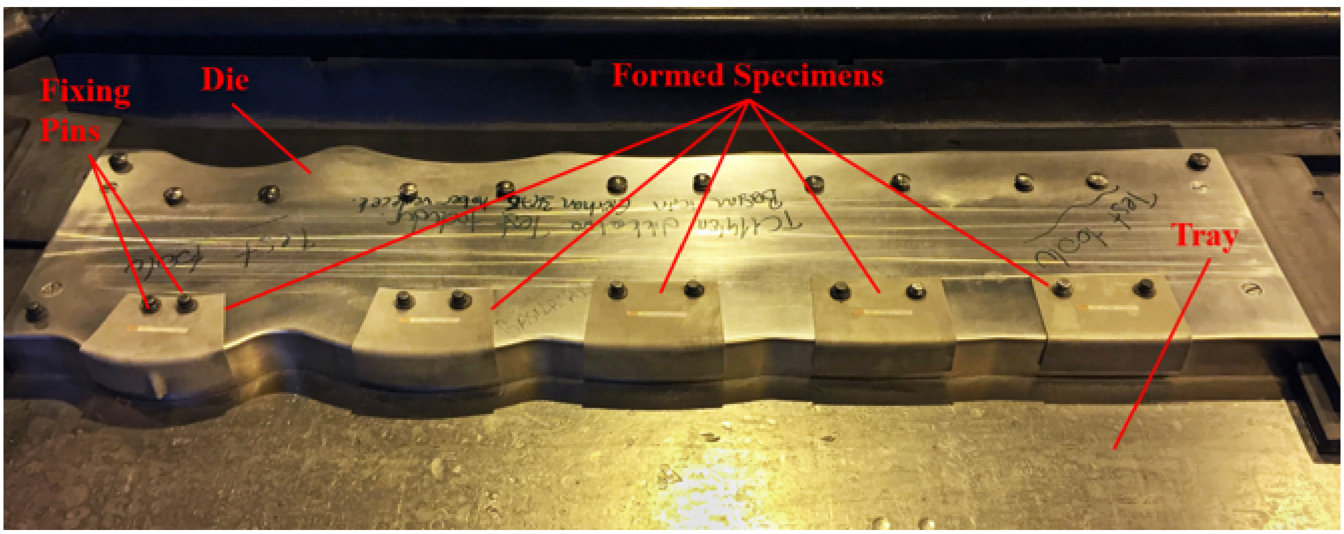


(b)

## Figure 7

a) Specimens and die used in the experiments b) Formed specimens


## Figure 8

Sample experiment result with two wrinkles (Al2024-W; T=1.27 mm; R=125 mm; F=40 mm)

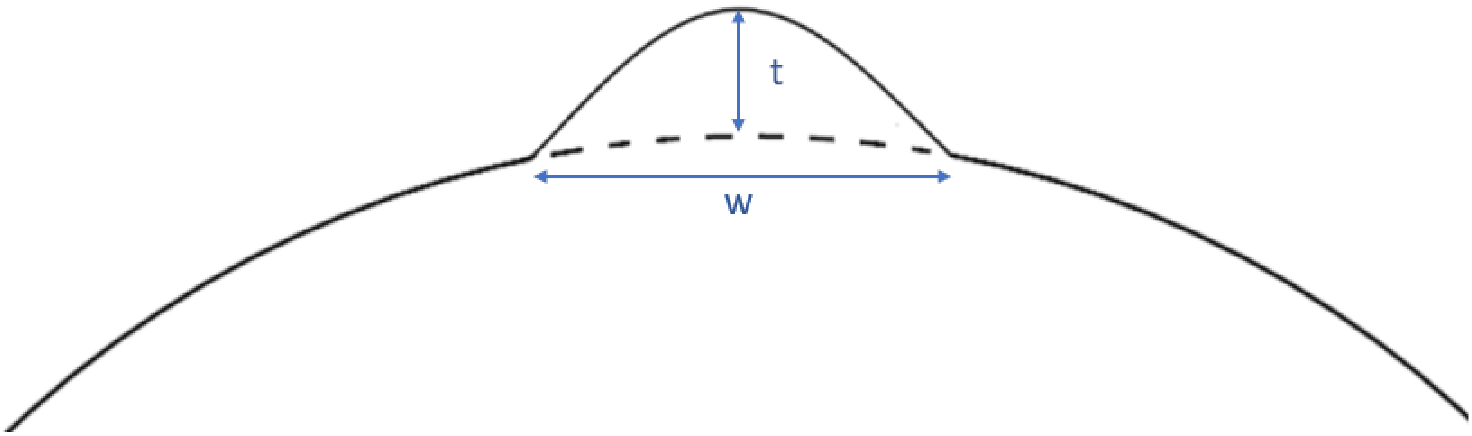


**Figure 9**

Schematic view of a wrinkle

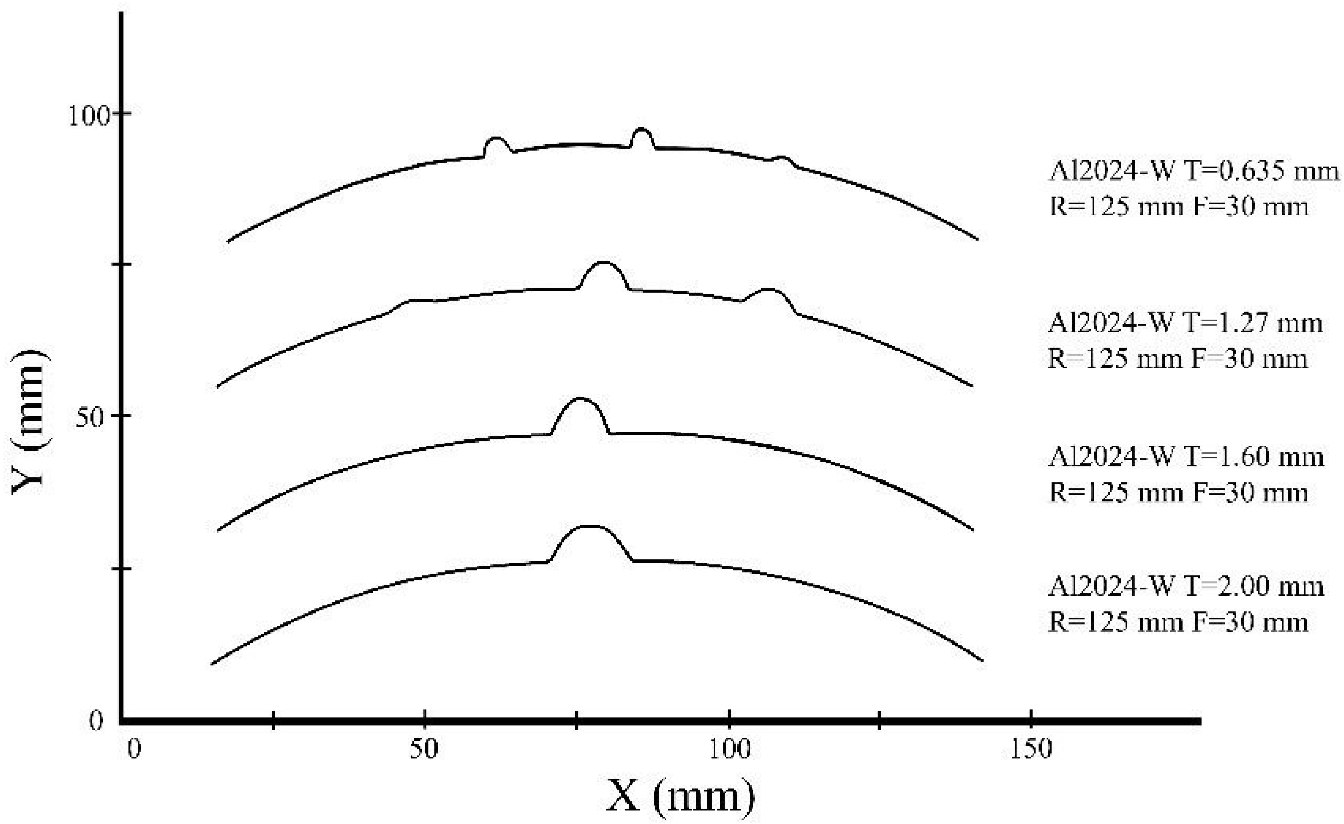


**Figure 10**

Effect of sheet thickness on wrinkling (AA2024-W, flange length: 30 mm, contour radius: 125 mm)

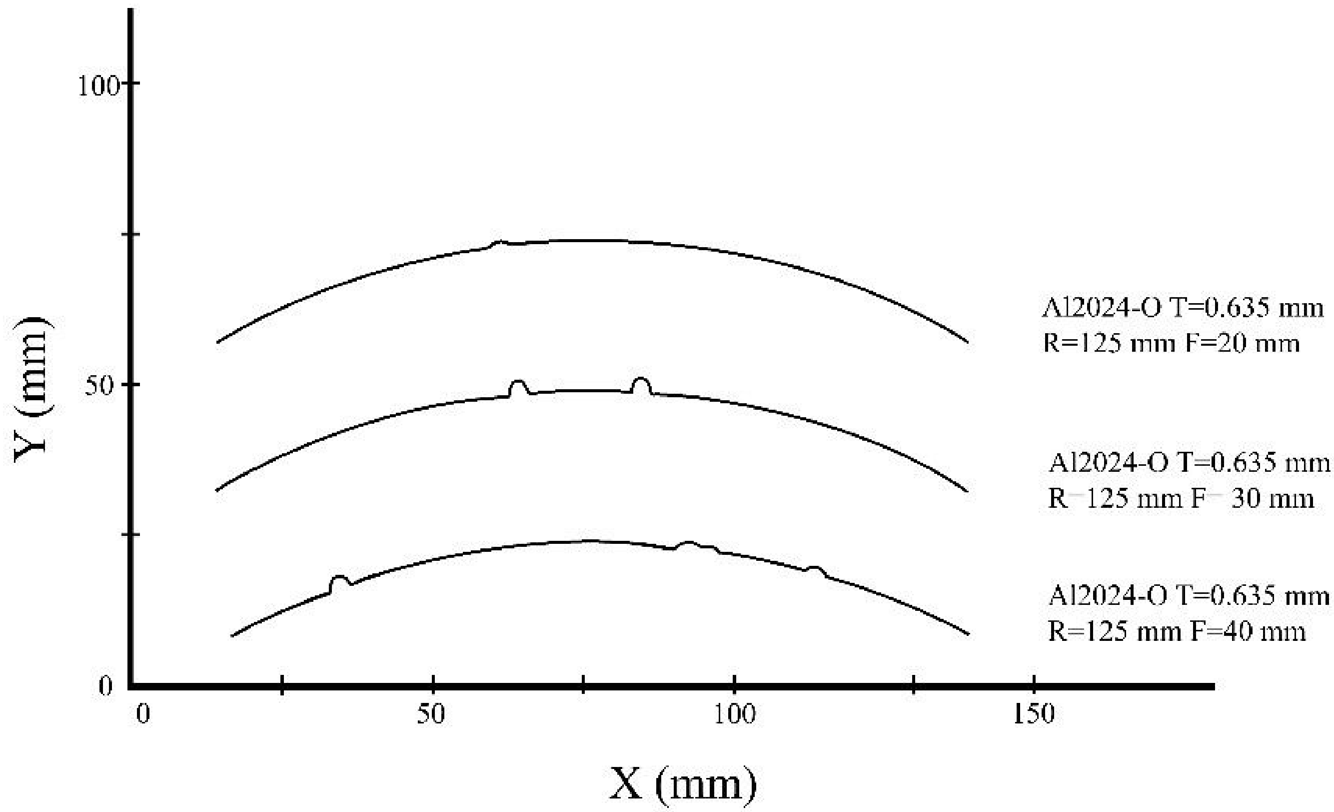


**Figure 11**

Effect of flange length on wrinkling (AA2024-O, thickness: 0.63 mm, contour radius: 125 mm)

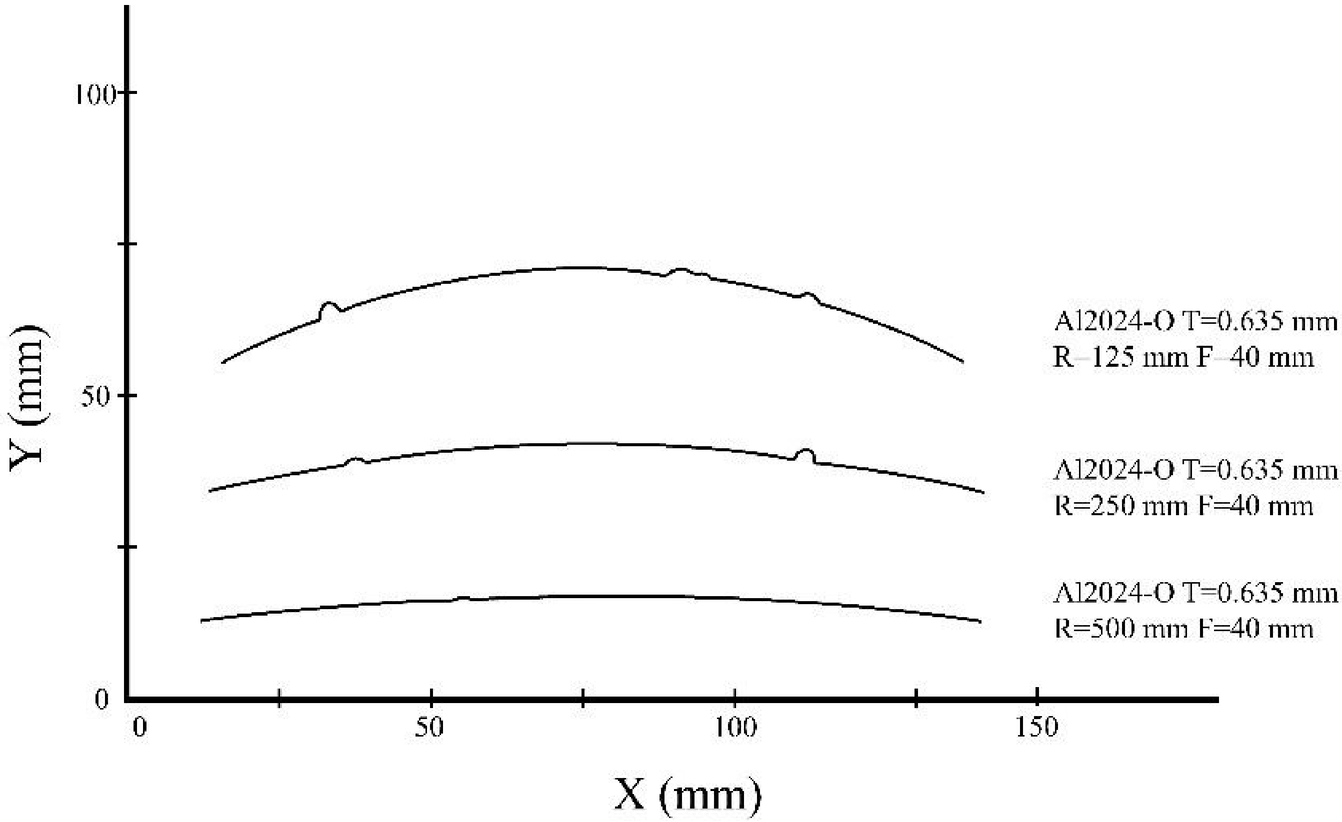


**Figure 12**

Effect of contour radius on wrinkling (AA2024-O, thickness: 0.63 mm, flange length 40 mm)

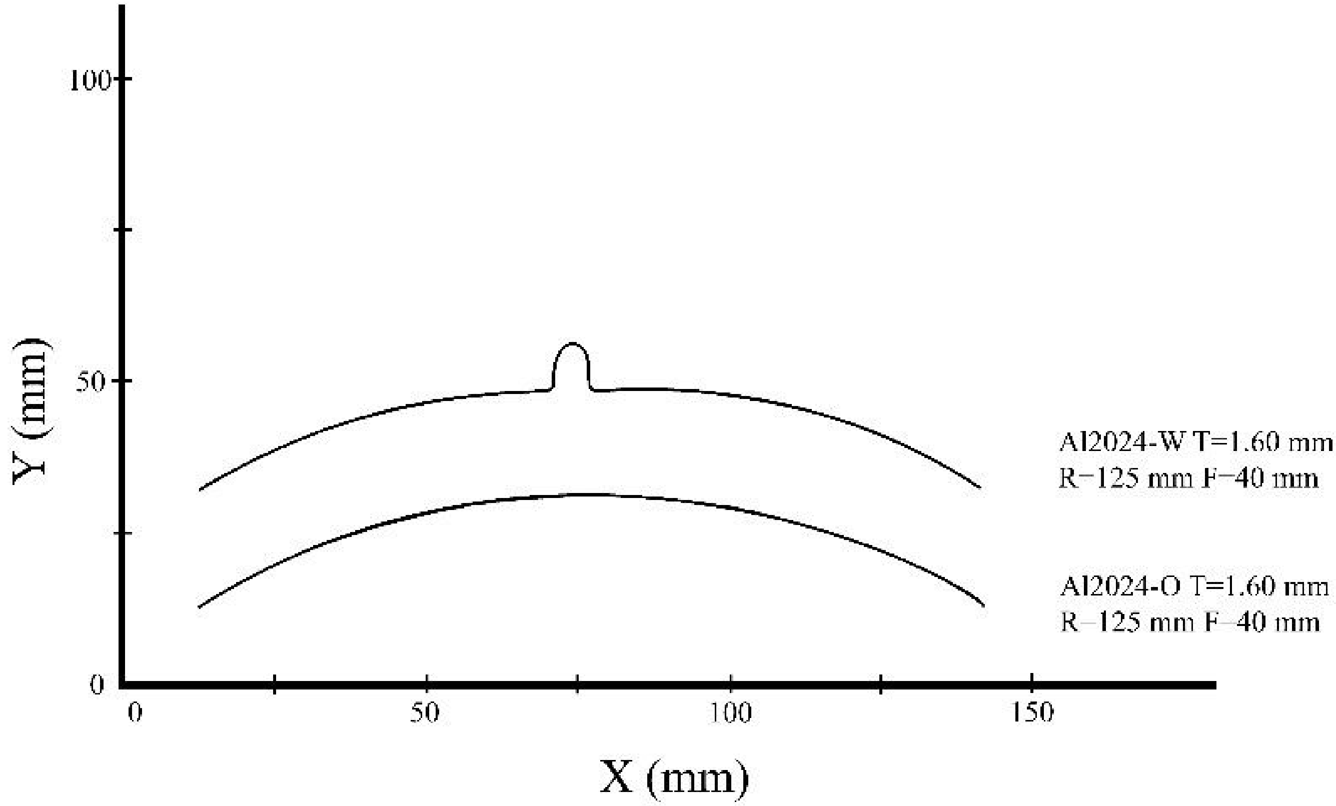


**Figure 13**

Effect of alloy condition on wrinkling (thickness: 0.63 mm, flange length: 40 mm, contour radius: 125mm)

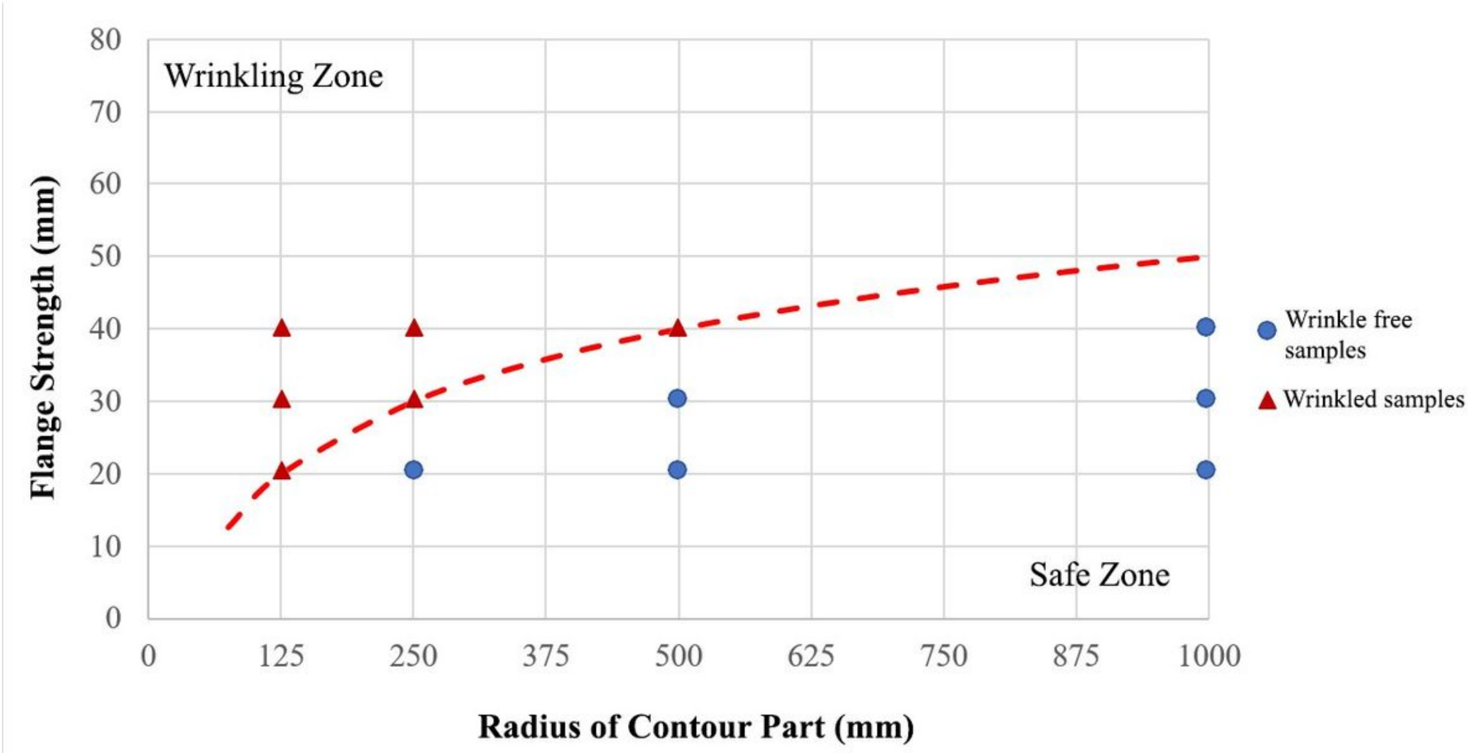


## Figure 14

Wrinkling Limit Diagram (WLD) for 0.63 mm thick AA2024-O